IEEE Photonics Journal
An IEEE Photonics Society Publication

Open Access

Bidirectional 4-PAM to Double Per-Fiber Capacity in 2-km Intra-Datacenter Links

Volume 10, Number 2, April 2018

Dario Pilori
Luca Bertignono
Antonino Nespola
Fabrizio Forghieri
Marco Mazzini
Roberto Gaudino

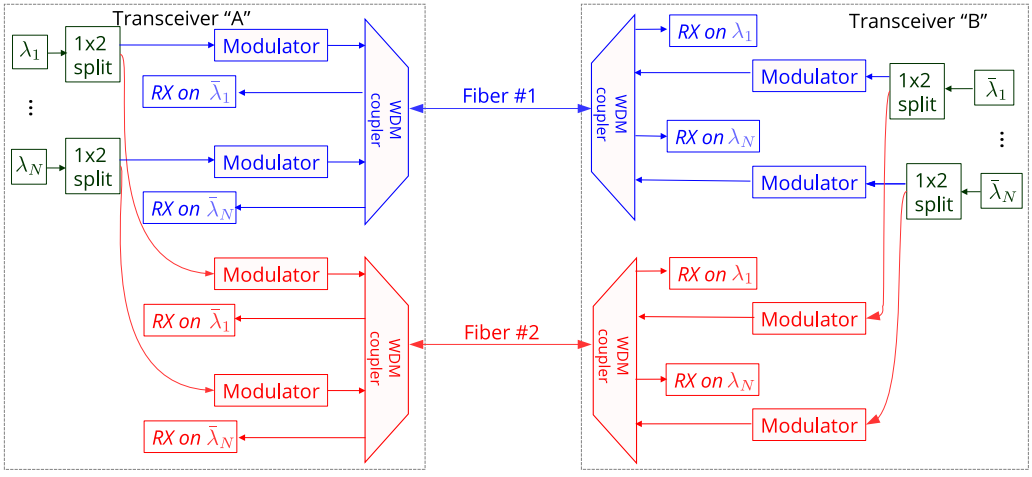

DOI: 10.1109/JPHOT.2018.2817195
1943-0655

Bidirectional 4-PAM to Double Per-Fiber Capacity in 2-km Intra-Datacenter Links

Dario Pilori,[1] **Luca Bertignono**,[1] **Antonino Nespola**,[2] **Fabrizio Forghieri**,[3] **Marco Mazzini**,[3] **and Roberto Gaudino** [1]

[1]DET, Politecnico di Torino, 10129 Torino, Italy
[2]Istituto Superiore Mario Boella, 10138 Torino, Italy
[3]Cisco Photonics Italy S.r.l., 20871 Vimercate, Italy

DOI:10.1109/JPHOT.2018.2817195

Manuscript received January 24, 2018; revised March 5, 2018; accepted March 15, 2018. Date of publication March 22, 2018; date of current version April 3, 2018. This work was partially sponsored by Cisco Photonics with an SRA contract. This paper was presented in part at the European Conference on Optical Communication, Gothenburg, September 2017. Corresponding author: Dario Pilori (e-mail: dario.pilori@polito.it).

Abstract: This paper presents an experimental demonstration of bidirectional 4-PAM transmission for intra-datacenter links using a pair of SMF fibers. In the proposed architecture, each transceiver laser feeds both fibers, which are thus used bidirectionally to double the capacity per used fiber, wavelength, and laser. Besides the experimental demonstration, we also report a theoretical and simulative investigation on the penalty induced in this architecture by spurious connector back-reflections. We show that the resulting penalty can be kept under control for typical realistic connector reflection values, provided that each pair of lasers in both directions are separated by at least twice the system symbol rate.

Index Terms: Pulse amplitude modulation (PAM), short-reach optical links, 100 Gb/s per wavelength transmission, datacenter interconnect.

1. Introduction

Recently, there have been a significant increase of interest towards Direct Detection (DD) M-PAM systems for short-reach (<2 km over SMF fibers) data-center applications [1]. In particular, the IEEE is in the progress of standardizing new high-speed Ethernet interfaces at 50-Gb/s and 100-Gb/s per wavelength, and even higher bit rate are expected in the near future. Anyway, future-generation Ethernet interfaces at speed higher than 100-Gb/s per wavelength per fiber will require significant increases in electronic device bandwidth and, consequently, cost; therefore, the research community in this field is looking for novel architectures to overcome these limitations without further increasing the symbol rate. Proposed solutions range from high-order modulation formats coupled with coherent detection [2], polarization division multiplexing with Stokes receivers [3] and single-sideband modulation coupled with discrete-multitone (DMT) modulation [4], [5]. Anyway, the cost of these solutions, which is acceptable for longer distances, is still perceived as impractical for <2-km intra-datacenter connections. Here, lasers are one of the key elements impacting transceiver cost: for instance, lasers on Silicon-Photonic platforms require expensive heterogeneous integration, and thus additional cost. In this scenario, an interesting metric is thus the bit rate delivered by each laser present inside a transceiver. Therefore, in this paper, we will propose and experimentally demonstrate a bi-directional architecture to double the capacity per laser in 4-PAM DD systems.

In particular, we assume to have a link made by two SMF fibers (one of today typical option inside top-level data centers), and we propose to use each of them bidirectionally over the same nominal wavelength grid. In particular, we propose a solution that, to reduce cost, uses twice each single laser, transmitting simultaneously on both fibers, and we investigate on the conditions under which the system can operate with small crosstalk penalty caused by spurious back-reflections. While short-reach bidirectional systems are not entirely novel, they are usually proposed using largely separated wavelengths, typically requiring lasers having two largely separated nominal wavelengths. Here, as a main result of our paper, we demonstrate that the wavelength spacing between counter-propagating wavelengths needs just to be slightly larger than twice the symbol rate. We remark that the main contribution of this paper is the bi-directional architecture, and not laser sharing inside a transceiver, which is a common architecture in different applications, such as transmit laser/local oscillator in coherent transceivers.

This paper greatly extends our previous work presented at ECOC 2017 [6], presenting a completely new theoretical assessment of the crosstalk-induced penalties caused by back-reflection on 4-PAM systems, and new (and more detailed) insights on the proposed architecture.

The paper is organized as follows. The proposed architecture is first described in details in Section II. Then, in Section III we derive a simple analytic expression to estimate the penalty from crosstalk, which inevitably arises in bi-directional schemes operating at the same nominal wavelength. The theoretical result is then validated with full time-domain numerical simulations. Then, in Section IV we present the experimental results proving the feasibility of the proposed architecture. Conclusions are drawn in Section V.

2. Proposed Bi-Directional System Architecture

A general schematic of the proposed architecture is shown in Fig. 1. In the transceiver, light generated by each laser is sent using 1×2 splitters to the two available SMFs which are used simultaneously for transmission of independent 4-PAM streams. This operation effectively doubles the capacity of the full system, at the expense of potential crosstalk penalties (which will be tackled in the next section), plus the unavoidable extra loss caused by the introduction of the splitters. Separation of the signals propagating in the two directions is performed by the WDM couplers, which requires properly isolated lasers.

As a rule-of-thumb power budget, the proposed system, compared to a mono-directional system, has an additional $\sim$3.5 dB loss due to the extra 1×2 splitter, plus the crosstalk penalty, which, as it will be shown later, can be kept below 0.5 dB under reasonable operating conditions. Overall, there is an $\sim$4 dB extra power budget requirement compared to a mono-directional system, while anyway doubling the overall bit rate. Other options to double the bit rate typically require much larger increase in power budget and/or cost. For instance, sticking with M-PAM only, doubling the 4-PAM bit rate keeping the same symbol rate requires moving to 16-PAM, which requires (at least) $\sim$7 dB more power than 4-PAM.

One of the key weakness of the proposed architecture is anyway the presence of back-reflections caused by link connectors, which have to be kept under control. For instance, legacy TIA-568 LC connectors, still widely used in data centers, have a maximum optical back-reflection specified as -26 dB. Moreover, in practical situations, a single "bad" connector may generate even higher back-reflections, thus giving stronger penalties.

To avoid those issues, we propose to *slightly* change the wavelength of each laser in one transceiver (indicated by $\bar{\lambda}_i$ in Fig. 1), e.g. by changing their temperature, while staying inside the specified wavelength grid tolerance $\Delta\bar{\lambda}$. While this option would be unpractical in Dense Wavelength Division Multiplexing (DWDM), it is actually feasible on the typical wavelength spacing used in short-reach links. For instance, assuming to adopt the Coarse Wavelength Division Multiplexing (CWDM) grid (G.694.2), $\Delta\lambda \approx 6 - 7$ nm, which corresponds to $\sim 1 - 1.2$ THz in the O-band. Adopting instead the narrower Ethernet LAN-WDM grid (4-nm spacing) [7], $\Delta\lambda$ is $\sim$2 nm (355 GHz). Nevertheless, even with the stricter LAN-WDM grid, a detuning by about twice the symbol rate (for instance 100–200 GHz for 100-Gb/s 4-PAM) is well inside the specified $\Delta\lambda$.

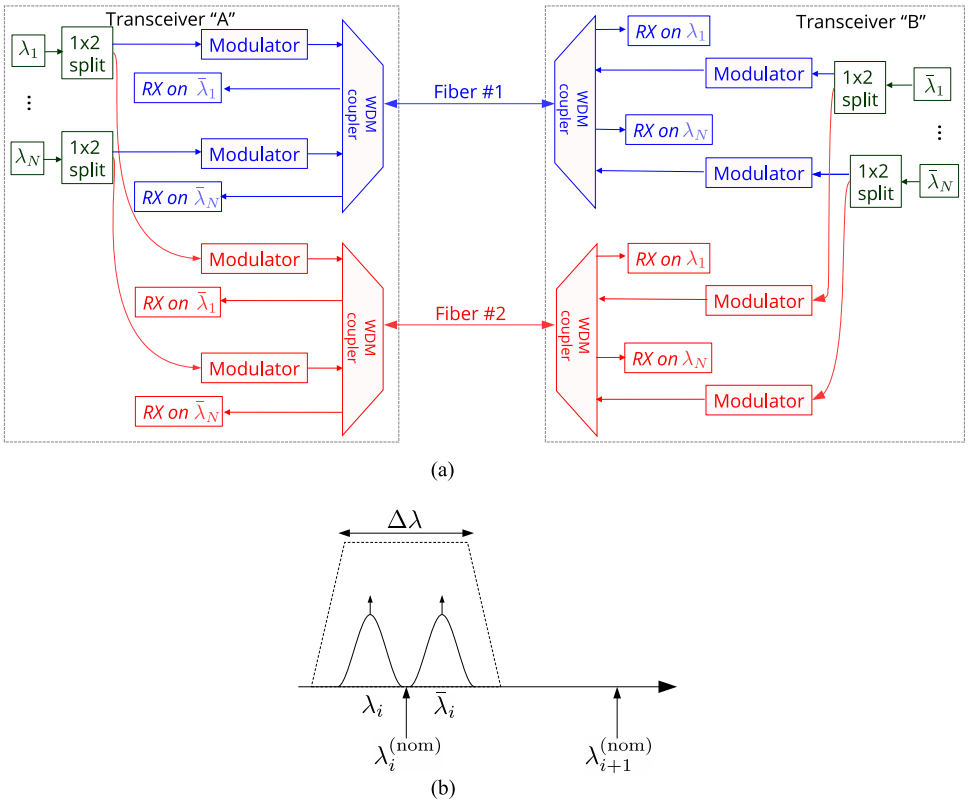

Fig. 1. General schematic of the proposed bidirectional architecture (a), where each fiber carries N Wavelength Division Multiplexing (WDM) 4-PAM channels in both directions. Optical spectrum of each fiber is shown in (b). Wavelengths λ_i and $\bar{\lambda}_i$ lay inside the wavelength tolerance of the i-th WDM channel $\Delta\lambda$ along the nominal wavelength $\lambda_i^{(\mathrm{nom})}$.

As a final comment on the proposed architecture, we point out that this solution does not require circulators, which are still critical components in integrated photonic circuits [8]–[10] since they have high insertion loss and are far to be commercially available. In conclusion, the proposed architecture is feasible, provided that crosstalk due to back-reflections is reduced by applying appropriate frequency shift on one of the lasers. To prove this, in the next Section III we will derive a simple theoretical model to evaluate the dependence between the magnitude of crosstalk and the laser detuning frequency. Then, in Section IV, the results will be experimentally demonstrated.

3. Impact of Crosstalk

The impact of crosstalk in IM/DD systems has been deeply studied in the past, but most of the investigations focused on binary On-Off Keying (OOK) modulation and on the interference of a signal with multiple delayed reflections of itself [11], [12]. In that scenario, which assumes numerous reflections, interference can be accurately approximated as Gaussian noise, allowing the use of simple equations to estimate the system-level impact of interference.

However, our proposed scenario is quite different, since it uses 4-PAM and, moreover, is typically impaired by a dominant single-reflection crosstalk generated by the worst-case connector of the link, which then creates interference on the signal propagating at the same nominal wavelength in the opposite direction. It has been shown [13] that the interference caused by one (or few) reflections cannot be accurately modeled as Gaussian noise, since this approximation was found to be overly pessimistic on system performance.

Therefore, in this section we will derive an analytical formula to evaluate performance for this particular case. The derivation will assume a simplified system model, similar to the model used in [13, Sec. II]. The main simplification is assuming "rectangular" 4-PAM signals in the time domain, received with a matched filter. This is the only condition that allows an analytical derivation of the problem. We will then analyze in the next sections a more realistic case of a severely band-limited 4-PAM received signal followed by an adaptive equalizer, first by simulation and then by experiments.

3.1 Theoretical Model

Let us consider a (time-domain) rectangular M-PAM optical signal, with an electric field

$$E_{\mathrm{tx}}(t) = \sqrt{x(t)} = \sqrt{\sum_{i=-\infty}^{+\infty} a_i \,\mathrm{rect}\left(\frac{t - iT}{T}\right)} \tag{1}$$

In this equation, a_k are the (positive) M-PAM levels, rect(.) is a rectangular pulse-shaping function, and $T = 1/R_S$ the symbol duration.

We assume that, in the received electric field, an interfering M-PAM signal $\sqrt{x_I(t)}\exp[j(2\pi\Delta f t + \phi(t))]$ is added with a given Signal-to-Interference Ratio (SIR), defined as the ratio between the optical power of the wanted and the interfering signals. While the two signals can interfere (in general) with arbitrary polarization, we will assume a worst-case situation where the signals are perfectly aligned in polarization. As shown in [14], this worst-case situation happens quite often in realistic systems. Moreover, we assume that the two transmitters are time synchronized. In case of unsynchronized transmitter, the interfering signal has (in general) lower amplitudes than a synchronized interferer, therefore we expect a smaller impact of interference. Nevertheless, specific simulations should be performed to properly justify this sentence, which are out of the scope of this work, and it will be discussed in future research.

Therefore, the received electric field can be expressed as:

$$E_{\mathrm{rx}}(t) = \sqrt{x(t)} + \sqrt{\frac{x_I(t)}{\mathrm{SIR}}} e^{j2\pi\Delta f t} e^{j\phi(t)} \tag{2}$$

where Δf is the frequency separation between two lasers and $\phi(t)$ represents a realization of laser phase noise.

After the photodiode (assumed ideal), the photocurrent $i(t)$ is proportional to

$$i(t) \propto x(t) + \frac{x_I(t)}{\mathrm{SIR}} + 2\sqrt{\frac{x(t)x_I(t)}{\mathrm{SIR}}}\cos\left(2\pi\Delta f t + \phi(t)\right) \tag{3}$$

From this equation, the sources of crosstalk have two different types of terms:

- The first source, which depends only on the SIR, is the so-called *incoherent* crosstalk. As long as Δf is smaller than the bandwidth of the WDM filter, this term cannot be removed.
- The second source is the so-called *coherent* crosstalk. As it will be shown later, for small values of Δf this term is the predominant source of crosstalk.

Therefore, to accurately evaluate the performance, it is crucial to understand how Δf and $\phi(t)$ influence the strength of coherent crosstalk. Assuming that:

- $i(t)$, after a DC-block, is filtered with an ideal matched filter (i.e. a rectangle) and sampled every T seconds.
- $\phi(t) = \phi_k$ is constant within one symbol.

We obtain the following signal for each symbol decision at the optimal sampling instant:

$$y(kT) = \frac{1}{T}\int_{(k-1)T}^{kT} i(t)\,\mathrm{d}t = a_k + \frac{a_k^{(I)}}{\mathrm{SIR}} + 2\sqrt{\frac{a_k a_k^{(I)}}{\mathrm{SIR}}}\cos\left[\phi_k\right]\frac{\sin(\pi\Delta f T)}{\pi\Delta f T} \tag{4}$$

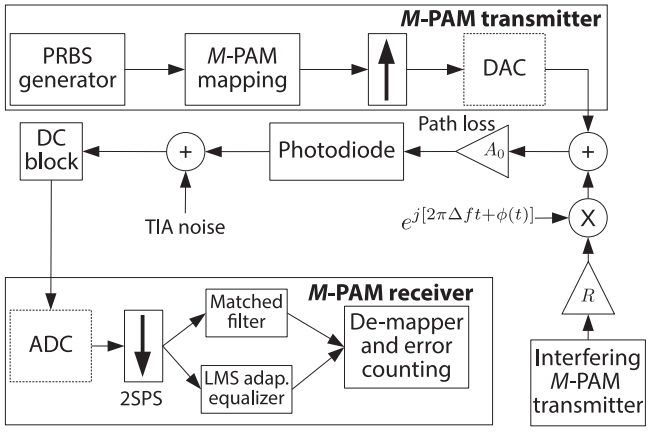

Fig. 2. Scheme of the time-domain simulation tool.

Before evaluating the Bit Error Rate (BER) performance, there are two random terms in (4) that have to be tackled: ϕ_k and $a_k^{(I)}$. Since both they are statistically independent from each other and from the transmitted symbol a_k, they can be averaged to obtain a deterministic formula. In particular, assuming that ϕ_k is uniformly distributed between 0 and 2π, then $\beta = \cos[\phi_k]$ has zero mean and the well-known probability distribution $f(\beta) = 1/\pi\sqrt{1-\beta^2}$ [15]. Then, assuming that $y(kT)$ is impaired by an Additive White Gaussian Noise (AWGN) (added by the Transimpedance Amplifier (TIA) at the receiver) with standard deviation σ_n, the probability of a symbol error given the transmitted symbol a_k and interfering symbol $a_k^{(I)}$ can be easily calculated from the well-known formula [16]

$$\mathcal{P}\left(e|a_k, a_k^{(I)}\right) = \frac{1}{2}\sum_i \mathbb{E}\left\{\operatorname{erfc}\left(\frac{\tilde{a}_k - \left[V_{\mathrm{th},i}^{(k)} + \frac{\tilde{a}_k^{(I)}}{\mathrm{SIR}} + 2\sqrt{\frac{a_k a_k^{(I)}}{\mathrm{SIR}}}\frac{\sin(\pi\Delta fT)}{\pi\Delta fT}\beta\right]}{\sqrt{2}\sigma_n}\right)\right\} \tag{5}$$

In this formula, the tilde ($\sim$) means removal of the mean value and the expectation has been performed over the random variable β. $V_{\mathrm{th},i}^{(k)}$ is the i-th decision threshold of the k-th symbol. In case of M-PAM, a symbol can either have two decision thresholds (upper and lower), or one.

Then, to calculate the SER, (5) needs to be averaged over all the possible transmitted and received symbols (assumed equiprobable)

$$\mathrm{SER} = \frac{1}{M^2}\sum_{k=1}^{M}\sum_{n=1}^{M}\mathcal{P}\left(e|a_k, a_n^{(I)}\right) \tag{6}$$

Finally, assuming Gray mapping, BER can be approximated as $\mathrm{BER} \approx \mathrm{SER}/\log_2 M$.

3.2 Simulation Tool

To validate both the theoretical formula and the experimental results of next section, we set up a full M-PAM time-domain simulation tool, whose scheme is summarized in Fig. 2.

A pseudo-random bit sequence is generated and mapped into an M-PAM constellation with a given extinction ratio. The signal is then upsampled with ideal rectangular pulses and (optionally) low-pass filtered by a Digital-to-Analog Converter (DAC). A random interfering M-PAM signal is generated, multiplied by a complex exponential $\exp[j(2\pi\Delta ft + \phi(t))]$ to emulate a different laser, scaled by the reflection R and added to the wanted signal. Note that, assuming that each M-PAM transmitter generates a signal with the same optical power, the reflection R is just the inverse of the SIR $R = \frac{1}{\mathrm{SIR}}$.

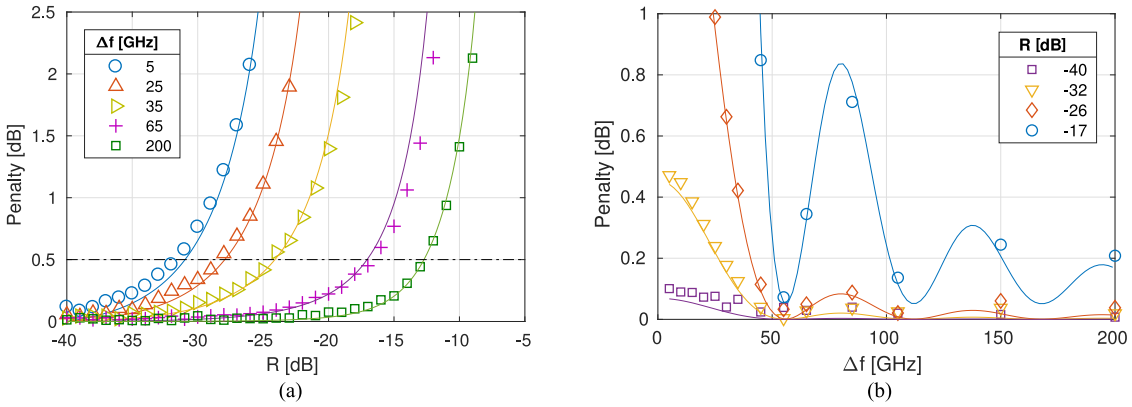

Fig. 3. Optical power penalty as a function of the reflection R for different values of laser spacing Δf (a) and as a function of the laser spacing for different values of reflection (b). Markers show results obtained with a full time-domain simulation of a 53 GBaud 4-PAM signal while solid lines are obtained with (5).

Due to the short distance and the use of O-band (typical for short-reach intra-datacenter links), chromatic dispersion is here neglected and fiber propagation is approximated as a lumped attenuation A_0. At the receiver, the signal is (optionally) low-pass filtered and quantized by an Analog-to-Digital Converter (ADC). Then, after downsampling at 2 samples per symbol, it can either be filtered by a static matched filter, or by a fractionally-spaced Least Mean Square (LMS) adaptive equalizer.

3.3 Validation and Discussion

To validate (5), we used the simulation tool of Fig. 2 to emulate the transmission of a 53 GBaud 4-PAM signal with ideal DAC and ADC and using a static matched-filter receiver. The extinction ratio was set to 10 dB.

A comparison between (5) and simulation results is shown in Fig. 3, as optical power penalty as a function of reflection R for different values of laser spacing Δf. The penalty has been calculated with respect to a baseline case with no interference ($R = -\infty$). The target BER is $2 \cdot 10^{-4}$ (KP4 FEC). It can be seen that the model is quite accurate, since it is able to predict with small errors the penalty in different conditions of reflection and frequency spacing. In the simulation, we assumed that the laser is Lorentzian with a 2-MHz linewidth.

Fig. 3(a) gives an important result on the feasibility of the proposed bidirectional 4-PAM system: crosstalk penalty increases for increasing back-reflections and for decreasing spectral separation Δf. Observing the actual numerical values, we can derive that for small values of Δf (e.g. 5 GHz), crosstalk impact is very high (due to the fact that the crosstalk appears as "coherent"), so that the maximum reflection value to have <0.5 dB power penalty is very low (-31.5 dB), a value not feasible with standard connector reflections (e.g. -26 dB for LC connectors). On the other end, increasing Δf above the symbol rate, the impact of crosstalk is strongly reduced, allowing much higher reflection values to have a <0.5 dB power penalty. For instance, at $\Delta f = 65$ GHz reflection can be as high as -17 dB, which is well inside the feasible on-field values of normal connectors. Fig. 3(b) shows the same simulation results of Fig. 3(a) as a function of the spectral separation. While coherent crosstalk is almost negligible for very small reflections (<-40 dB), for stronger values (such as -26 dB) spectral separation needs to be greater than (at least) the symbol rate to have a stable power penalty below 0.5 dB. For strong reflections, power penalty strongly fluctuates with Δf due to the overlap between the side lobes of the interfering signal with the signal under test. Mathematically, this is explained by the $\sin(\pi \Delta f T)/(\pi \Delta f T)$ term of (5).

Therefore, from this theoretical investigation we can conclude that, if Δf is "large enough" compared to the symbol rate, the impact of crosstalk is limited, and a bidirectional system with this

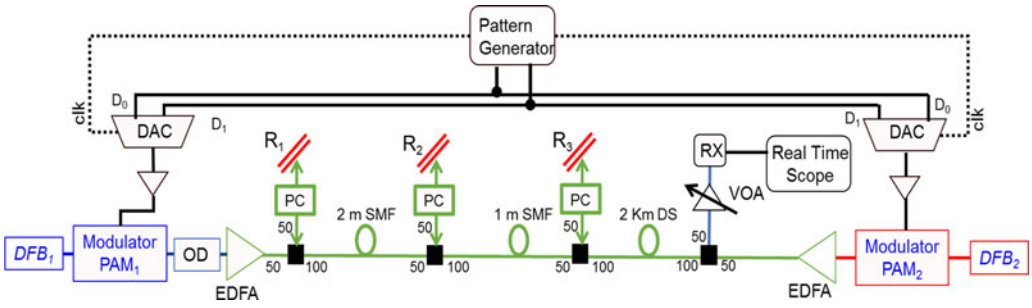

Fig. 4. Experimental setup.

value of Δf can tolerate back-reflections from standard connectors. This result is strongly related to the case that the receiver electrical filter has a bandwidth of the order of R_s, so that for $\Delta f > R_s$ the resulting coherent crosstalk beating term is significantly attenuated by the filter itself. However, realistic short reach systems often have strong bandwidth limitations at the DAC, optoelectronics and ADC level, which then have to be tackled with adaptive equalization. Consequently, the hypothesis used to derive (5) does not hold anymore. Our current conclusion has thus still to be confirmed using experiments, as it is done in the following section.

4. Experimental Validation

4.1 Setup

To validate the feasibility of the proposed bi-directional system, we set up an experimental system depicted in Fig. 4. Since the purpose of this work is the investigation of crosstalk penalty at the same nominal wavelength, we performed only single-channel bidirectional transmission.

A 4-PAM transmitter, operating either at 53 or 28 GBaud, modulates two Distributed FeedBack (DFB) lasers (with a $\sim$2 MHz linewidth) using a pair of 33-GHz lithium-niobate optical modulators. The two data paths are delayed by approximately 400 symbols to decorrelate the two 4-PAM signals. Two Erbium Doped Fiber Amplifiers (EDFAs) are inserted at each transmitter side, with the sole purpose of recovering the insertion loss of the optical modulators. It should be noted that, due to the very limited propagation distance and thus fiber loss, ASE noise added by these EDFAs was negligible, generating very high values of optical Signal to Noise Ratio (SNR) which we verified that is giving an almost null impact on performance, which is actually limited by receiver thermal noise, as in any typical commercial transceiver for this application scenario. Moreover, due to the unavailability of O-band components in our lab, the experiment was set up in C-band with some modifications to emulate O-band transmission. In particular, propagation is performed over a 2-km span of Dispersion Shifted (DS) fiber, which has approximately the same chromatic dispersion at 1550 nm as an SMF used in the in O-band. The receiver is a standard PIN photodiode (with a TIA for 53 GBaud transmission) connected to a 50 GS/s (or 100 GS/s for 53 GBaud) real-time oscilloscope. Receiver DSP, performed offline, used a typical 10-tap LMS adaptive equalizer.

Back-reflections are emulated by (up to) three lumped reflectors (shown as R_1, R_2 and R_3 in Fig. 4) connected to the main transmission fiber using 1×2 couplers and Polarization Controllers (PCs) to align the polarization of the reflected signal to the polarization of the incoming signal. The values of the reflections have been normalized to the loss of the couplers, so that it is equal to the inverse of the SIR ($R = 1/\text{SIR}$).

4.2 Single Reflector

As discussed in Section II, the most typical source of interference in the considered link scenario is a back-reflection generated by a single “bad” connector which causes interference between the wanted 4-PAM signal and the signal transmitted in the opposite direction. Therefore, we emulated

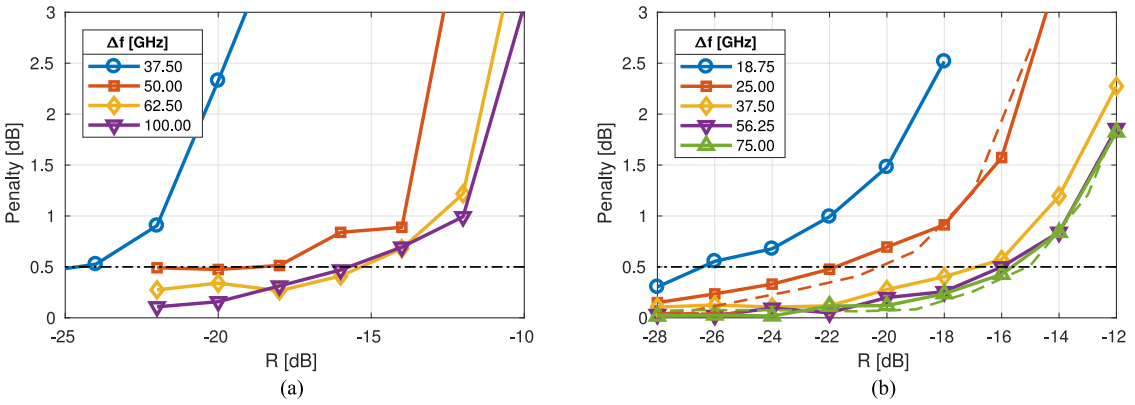

Fig. 5. Experimental results with a single reflection, as optical power penalty as a function of the reflection R, for 4-PAM transmission at 53 GBaud (a) and 28 GBaud (b). Dashed lines in (b) are numerical simulations obtained with simulator in Fig. 2.

these conditions using a single reflector R_3; we measured the BER of the wanted PAM_1 signal, while changing the power of the reflection of the interfering PAM_2 signal and the frequency difference between the two lasers Δf by thermal tuning of the DFBs.

In Fig. 5 we show the optical power penalty at 53 GBaud (a) and 28 GBaud (b) versus reflections values in dB, for different spectral separation Δf. While for small values of Δf (compared to the symbol rate) the maximum tolerable reflection is lower than back-reflections of standard LC connectors (-26 dB), by increasing Δf (at least) above the symbol rate the maximum tolerable reflection becomes higher. For instance, at 53 GBaud, for $\Delta f \geq 62.5$ GHz, the maximum acceptable reflection is -15.5 dB, which is a well inside the value specified for standard LC connectors.

To validate the experimental results we performed a numerical simulation, using the simulation tool detailed in Section III-B, numerically emulating the same receiver structure and imposing the same DAC and ADC bandwidth limitations (one-pole filter with $f_{3dB} = 23$ GHz). Results are shown as dashed lines in Fig. 5(b) for two different values of Δf (25 and 75 GHz). As shown in the figure, there is a good agreement between the two results, thus cross-validating the conclusions drawn from the experimental results.

4.3 Multiple Reflections

In our proposed bi-directional architecture (Fig. 1), as stated in Section II, the most important cause of crosstalk are typically single-reflector back-reflections. However, multiple reflections, even if they happen only in presence of several "bad" connectors, can be particularly detrimental due to the coherent accumulation of crosstalk.

To test these conditions, using the same experimental setup of Fig. 4, we measured the BER of the wanted PAM_1 with three (R_1, R_2 and R_3) reflections of PAM_2. Results are shown in Fig. 6, where the optical power penalty is shown as a function of the total reflection $R = R_1 + R_2 + R_3$. The values of each reflection (R_1, R_2 and R_3) have been chosen such that the power of each of them is equal at the receiver.

In presence of multiple reflections, the total reflected power and the relative phase among the spurious signal is highly random, giving rise to time-fluctuating BER. Therefore, to be conservative on our experimental analysis, for each point in Fig. 6 we measured the BER of 100 different two-million-samples sequences captured by the real-time oscilloscope, and we kept the *worst* measure of every point.

Fig. 6 shows results at 28 GBaud for two different laser spacing: $\Delta f = 25$ GHz (dashed lines) and $\Delta f = 56.25$ GHz (solid lines) with one (R_3, circles) and three reflections (squares). While the total reflection is the same, results with three reflections are $\sim$4 dB worse with both values of Δf. Multiple reflections make interference noise closer to be Gaussian-distributed, which introduce

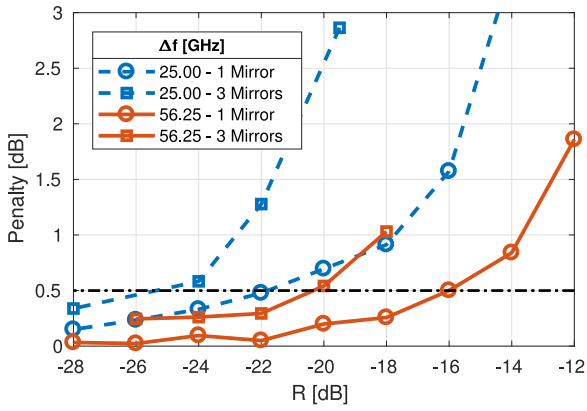

Fig. 6. Experimental results with one (circles) and three (squares) reflections. The optical power penalty is measured a function of the total reflection R, for 4-PAM transmission at 28 GBaud.

worse penalties than a single interfering 4-PAM signal, a result that for binary OOK was actually already well-known, see for instance [13], and which we confirm here also for 4-PAM.

Therefore, the presence of multiple reflections require larger values of Δf. In particular, from the results of Fig. 6, we should set $\Delta f \geq 56.25$ GHz (which is approximately twice the symbol rate) to have a maximum acceptable total reflection of -20 dB.

5. Conclusion

In this work, we proposed a bidirectional architecture to double per-fiber and per-laser capacity in M-PAM short-reach optical links. To avoid the detrimental effect of crosstalk introduced by connector back-reflections, we proposed a proper laser frequency detuning while still keeping the lasers inside WDM optical filter bandwidths. Using an analytic model, numerical simulations and an experimental validation, we found that, if the frequency detuning is approximately larger than twice the symbol rate, the optical power penalty due crosstalk can be kept below 0.5 dB under very realistic requirements for spurious back-reflections coming from connectors or component interfaces. This result has been obtained assuming time synchronization between the two interfering transmitter. While we do not expect different conclusions for unsynchronized transmitters, future research should properly investigate this case.

In order to make this system feasible, future work should implement an automatic wavelength tracking control to tune the laser wavelengths ensuring that Δf is large enough to keep a small crosstalk penalty but at the same time stay inside the CWDM or LAN-WDM receiver filters tolerances.

Acknowledgment

The authors would like to thank Oclaro for lending the optical modulators used in this experiment and the PhotoNext Interdepartmental Center at Politecnico di Torino (www.photonext.polito.it).

References

[1] S. Bhoja, "PAM4 signaling for intra-data center and data center to data center connectivity (DCI)," in *Proc. Optical Fiber Commun. Conf., Optical Soc. Amer.*, 2017, Paper W4D.5.

[2] R. Emmerich *et al.*, "Colorless C-band WDM system enabled by coherent reception of 56-GBd PDM-16QAM using an high-bandwidth ICR with TIAs," in *Proc. Optical Fiber Commun. Conf., Optical Soc. Amer.*, 2017, Paper M2C.3.

[3] D. Che, A. Li, X. Chen, Q. Hu, Y. Wang, and W. Shieh, "160-Gb/s stokes vector direct detection for short reach optical communication," in *Proc. Optical Fiber Commun. Conf., Postdeadline Papers., Optical Soc. Amer.*, 2014, Paper Th5C.7.

[4] S. Randel, D. Pilori, S. Chandrasekhar, G. Raybon, and P. Winzer, "100-Gb/s discrete-multitone transmission over 80-km SSMF using single-sideband modulation with novel interference-cancellation scheme," in *Proc. Eur Conf. Opt. Commun*., 2015, pp. 1–3.
[5] D. Pilori, C. Fludger, and R. Gaudino, "Comparing DMT variants in medium-reach 100G optically amplified systems," *J. Lightw. Technol.*, vol. 34, no. 14, pp. 3389–3399, Jul. 2016.
[6] A. Nespola, L. Bertignono, D. Pilori, F. Forghieri, M. Mazzini, and R. Gaudino, "Bidirectional PAM-4 experimental proof-of-concept to double capacity per fiber in 2-km data center links," in *Proc. Eur. Conf. Opt. Commun*., 2017, Paper P2.SC5.1.
[7] Standard for Ethernet, IEEE Standard 802.3-2015, 2015.
[8] C. R. Doerr, L. Chen, and D. Vermeulen, "Silicon photonics broadband modulation-based isolator," *Opt. Exp.*, vol. 22, no. 4, pp. 4493–4498, Feb. 2014.
[9] P. Pintus, F. D. Pasquale, and J. E. Bowers, "Integrated TE and TM optical circulators on ultra-low-loss silicon nitride platform," *Opt. Exp.*, vol. 21, no. 4, pp. 5041–5052, Feb. 2013.
[10] K. Mitsuya, Y. Shoji, and T. Mizumoto, "Demonstration of a silicon waveguide optical circulator," *IEEE Photon. Technol. Lett.*, vol. 25, no. 8, pp. 721–723, Apr. 2013.
[11] C. R. Fludger, M. Mazzini, T. Kupfer, and M. Traverso, "Experimental measurements of the impact of multi-path interference on PAM signals," in *Proc. Optical Fiber Commun. Conf., Optical Soc. Amer.*, 2014, Paper W1F.6.
[12] J. L. Gimlett and N. K. Cheung, "Effects of phase-to-intensity noise conversion by multiple reflections on gigabit-per-second DFB laser transmission systems," *J. Lightw. Technol*., vol. 7, no. 6, pp. 888–895, Jun. 1989.
[13] J. C. Attard, J. E. Mitchell, and C. J. Rasmussen, "Performance analysis of interferometric noise due to unequally powered interferers in optical networks," *J. Lightw. Technol*., vol. 23, no. 4, p. 1692, Apr. 2005.
[14] E. L. Goldstein, L. Eskildsen, C. Lin, and Y. Silberberg, "Polarization statistics of crosstalk-induced noise in transparent lightwave networks," *IEEE Photon. Technol. Lett*., vol. 7, no. 11, pp. 1345–1347, Nov. 1995.
[15] A. Papoulis and S. U. Pillai, *Probability, Random Variables, and Stochastic Processes*. New York, NY, USA: Tata McGraw-Hill Education, 2002.
[16] J. Proakis and M. Salehi, *Digital Communications*, 5th ed. New York, NY, USA: McGraw-Hill, 2007.